






A Trojan Horse Approach to the Production of ^{18}F in Novae

M. La Cognata¹ , R. G. Pizzone¹, J. José^{2,3} , M. Hernanz^{3,4} , S. Cherubini^{1,5}, M. Gulino^{1,6},
G. G. Rapisarda^{1,5}, and C. Spitaleri^{1,5}

¹ INFN—Laboratori Nazionali del Sud, Catania, Italy; lacognata@lns.infn.it

² Departament de Física, EEBE, Universitat Politècnica de Catalunya, E-08019 Barcelona, Spain

³ Institut d'Estudis Espacials de Catalunya, E-08034 Barcelona, Spain

⁴ Institut de Ciències de l'Espai (ICE-CSIC). Campus UAB. c/ Can Magrans s/n, E-08193 Bellaterra, Spain

⁵ Dipartimento di Fisica e Astronomia, Università degli Studi di Catania, Catania, Italy

⁶ Facoltà di Ingegneria ed Architettura, Kore University, Viale delle Olimpiadi, 1, I-94100 Enna, Italy

Received 2017 May 10; revised 2017 July 31; accepted 2017 August 3; published 2017 August 31

Abstract

Crucial information on nova nucleosynthesis can be potentially inferred from γ -ray signals powered by ^{18}F decay. Therefore, the reaction network producing and destroying this radioactive isotope has been extensively studied in the last years. Among those reactions, the $^{18}\text{F}(p, \alpha)^{15}\text{O}$ cross-section has been measured by means of several dedicated experiments, both using direct and indirect methods. The presence of interfering resonances in the energy region of astrophysical interest has been reported by many authors including the recent applications of the Trojan Horse Method. In this work, we evaluate what changes are introduced by the Trojan Horse data in the $^{18}\text{F}(p, \alpha)^{15}\text{O}$ astrophysical factor recommended in a recent R-matrix analysis, accounting for existing direct and indirect measurements. Then the updated reaction rate is calculated and parameterized and implications of the new results on nova nucleosynthesis are thoroughly discussed.

Key words: gamma rays: stars – novae, cataclysmic variables – nuclear reactions, nucleosynthesis, abundances

1. Introduction

Classical novae are thermonuclear explosions occurring in the envelopes of accreting white dwarfs in stellar binary systems. The material transferred by the companion accumulates on top of the white dwarf under degenerate conditions, driving a thermonuclear runaway. The energy unleashed by the set of nuclear processes acting in the envelope heats the material up to peak temperatures of $\sim(1-4) \times 10^8$ K. During these events, about 10^{-3} – $10^{-7} M_{\odot}$, enriched in CNO and, sometimes, other intermediate-mass elements (e.g., Ne, Na, Mg, Al) are ejected into the interstellar medium (see José & Shore 2008; Starrfield et al. 2008, 2016; José 2016 for recent reviews). While classical novae have been observed in all wavelengths, spanning from radio-waves to high-energy γ -rays (with $E > 100$ MeV), they have been quite elusive in the ~ 0.1 – 1 MeV range, where emission from few radioactive nuclei is predicted.

The role of classical nova outbursts as potential sources of γ radiation was first reviewed by Clayton & Hoyle (1974) and Clayton (1981). Two types of emission are expected. The early (or prompt) γ -ray emission (511 keV line plus continuum) is driven by the disintegration of the short-lived, β -unstable isotopes ^{13}N and ^{18}F . The decay of other medium-lived radioactive species, such as ^7Be and ^{22}Na , into excited states of their daughter nuclei and the following de-excitation by emission of a γ -ray photon of definite energy (478 keV for ^7Be , 1275 keV for ^{22}Na) generates late γ -ray emission. Classical novae are also predicted to be partly responsible for the overall Galactic 1809 keV ^{26}Al line (see Hernanz 2008, 2014 for recent reviews).

At the physical conditions that characterize nova envelopes, the positrons emitted in the β^+ -decays of ^{13}N and ^{18}F should thermalize before they annihilate with the surrounding electrons (Leising & Clayton 1987). Only $\sim 10\%$ of the released positrons directly annihilate, while the vast majority $\sim 90\%$ is expected to form positronium, a system made up of an electron and a positron bound together. Models suggest

that one-fourth of the positronium atoms form in singlet state (or para-positronium), characterized by antiparallel electron–positron spins and a mean lifetime of $\tau = 125$ ps. In this configuration, positronium preferentially decays by emitting two 511 keV γ -ray photons (in fact, para-positronium decay can emit any even number of photons, but with lower probability as the number of photons rises). The other positronium atoms settle in a triplet state configuration (or ortho-positronium), with parallel spins and a mean lifetime of $\tau = 145$ ns, which preferentially decay producing three γ -ray photons, each with an energy below 511 keV. The prompt γ -ray emission expected for novae is composed of a 511 keV line (fed by direct electron–positron annihilation) and a lower-energy continuum (supplied by positronium decay plus Comptonization of 511 keV photons; see Leising & Clayton 1987; Gómez-Gomar et al. 1998; Hernanz et al. 1999), with a cut-off at ~ 20 – 30 keV due to photoelectric absorption. The existence of such a sharp cut-off precludes the possibility that the hard X-ray flux observed in novae may result from Compton degradation of γ -rays, as indicated in a number of papers (see, e.g., Livio et al. 1992; Suzuki & Shigeyama 2010). It is worth observing that this is the most powerful γ -ray emission predicted for classical novae (Leising & Clayton 1987; Gómez-Gomar et al. 1998; Hernanz et al. 1999).

Despite the relatively large fluxes expected for this prompt emission, its detection represents a real challenge, as it occurs well before the nova is discovered by optical means. This rules out any chance of repointing a γ -ray satellite once a nova has been singled out. Accordingly, any possibility relies solely on a posteriori data analysis, on the track of γ -ray excess release around 511 keV from the direction of novae after their optical observation. To this purpose, data obtained with the TGRS instrument on board the *WIND* satellite (Harris et al. 1999), with the BATSE instrument on board the Compton Gamma-Ray Observatory (Hernanz et al. 2000), or with the *RHESSI* satellite (Matthews et al. 2006), has been analyzed; however,

only upper limits on the ^{18}F annihilation line have been set to date. Current estimates of the maximum detectability distance of the 511 keV line with the SPI spectrometer on board the γ -ray observatory *INTEGRAL* return a value of ~ 3 Kpc (Hernanz et al. 1999; Hernanz & José 2004). Nonetheless, such evaluations critically depend on an accurate knowledge of the various nuclear processes involved in the destruction and production of ^{18}F during nova outbursts.

Production of ^{18}F in novae is triggered by the $^{16}\text{O}(p, \gamma)^{17}\text{F}$ reaction, which is either followed by $^{17}\text{F}(p, \gamma)^{18}\text{Ne}(\beta^+)^{18}\text{F}$ or by $^{17}\text{F}(\beta^+)^{17}\text{O}(p, \gamma)^{18}\text{F}$. Owing to the relatively large half-life of ^{18}F ($T_{1/2} = 110$ minutes), it is mainly burnt by proton-captures, predominantly by $^{18}\text{F}(p, \alpha)^{15}\text{O}$, and to a smaller extent by $^{18}\text{F}(p, \gamma)^{19}\text{Ne}$ (see, e.g., José 2016). For nova conditions, the most uncertain reaction of the network of nuclear processes cited above is, by far, $^{18}\text{F}(p, \alpha)^{15}\text{O}$. In the last decade, this reaction has been extensively studied and, in particular, many investigations have focused on its examination by means of direct measurements at the relevant astrophysical energies. Such experimental studies are very challenging not only for the energy range of interest, which leads to vanishingly small cross-sections, but also for the reason that ^{18}F is a radioactive isotope, so it requires dedicated facilities to be synthesized. Starting from the beginning of this century, many experimental collaborations have attempted to measure the $^{18}\text{F}(p, \alpha)^{15}\text{O}$ astrophysical S(E)-factor. A first direct experiment was performed by Bardayan et al. (2002), focusing on the resonance at $E_{c.m.} = 330$ keV and its strength. Afterward, additional experimental investigations were performed by many groups using different experimental approaches, see e.g., De Sereville et al. (2009), Beer et al. (2011), and Laird et al. (2013). So far, many uncertainties are still present on the low-energy resonances, their widths and interference, thus influencing the evaluation of the reaction rate at the temperatures relevant for astrophysics and, consequently, the nova nucleosynthesis. Therefore, new experimental studies, especially centered at the nova Gamow window, are mandatory.

2. THM Basic Features and Application to the $^{18}\text{F}(p, \alpha)^{15}\text{O}$ Reaction

Alternative and valuable approaches to obtain the bare-nucleus cross-section (devoid of electron screening effects), σ_b , for charged particles at energies lower than the Coulomb barrier, have been made available by indirect methods. Among them, the Trojan Horse Method (THM; Spitaleri 1991) is well suited to study binary reactions induced at astrophysical energies by neutrons or charged particles by using convenient reactions with three particles in the exit channel. THM enables us to by-pass both Coulomb barrier suppression and electron screening enhancement, thus making the use of extrapolation unnecessary. In the last two decades, the method has turned out to be very profitable in the application to several aspects of nuclear astrophysics research, such as primordial nucleosynthesis (Pizzone et al. 2014; Tumino et al. 2014), the lithium problem (Pizzone et al. 2005; Lamia et al. 2013), AGB nucleosynthesis (Palmerini et al. 2013; La Cognata et al. 2015), and light-element depletion in stars (Lamia et al. 2015). In all of these cases, the THM has been applied to the study of reactions between stable nuclei and p , α , or, more recently, neutrons (Gulino et al. 2013). Therefore, the method can be considered to be a robust indirect technique to deduce a bare-

nucleus cross-section for reactions of astrophysical interest, leading to the establishment of accurate reaction rates.

The basic premises of the THM have recently been reviewed in Tribble et al. (2014) and Spitaleri et al. (2016). Here we shall just underscore that it is based on the quasi-free (QF) breakup reaction mechanism, which enables us to indirectly derive the astrophysical factor of a binary process from the measurement of a suitable three-body one. In particular, the QF reaction mechanism specializes in the THM approach, relevant for astrophysical applications. When the energy of the incident particle is chosen large enough to overcome the Coulomb barrier of the interacting nuclei, the breakup of the TH nucleus into a participant and a spectator particle can be regarded as occurring within the nuclear interaction field, so that Coulomb repulsion is greatly suppressed. As a consequence, the THM also becomes insensitive to problems connected with the electron screening, the interaction energies being well above the typical energies at which the atomic degrees of freedom can play a role.

In this paper, we will describe an R-matrix analysis of the recent THM measurements of the $^{18}\text{F}(p, \alpha)^{15}\text{O}$ cross-section, addressing the open questions making the reaction rate more uncertain at the lower temperatures, because of unknown properties of near-threshold resonances and interference between these and higher energies broad states.

The THM was applied to the $^2\text{H}(^{18}\text{F}, \alpha^{15}\text{O})n$ process to obtain critical information regarding the $^{18}\text{F}(p, \alpha)^{15}\text{O}$ cross-section at energies of astrophysical interest, below about 400 keV (Cherubini et al. 2015; Pizzone et al. 2016). In the $^2\text{H}(^{18}\text{F}, \alpha^{15}\text{O})n$ reaction, the QF breakup was identified and selected, with deuteron splitting into its constituents p and n , whereby n is regarded as the spectator to the $^{18}\text{F}(p, \alpha)^{15}\text{O}$ virtual reaction.

According to the Plane Wave Impulse Approximation, the differential cross-section of the $2 \rightarrow 3$ reaction measured in a α - ^{15}O coincidence experiment can be expressed in a form explicitly featuring the cross-section of the binary virtual reaction:

$$\frac{d^3\sigma}{dE_\alpha d\Omega_\alpha d\Omega_{^{15}\text{O}}} \propto \text{KF} |\Phi(\mathbf{p}_s)|^2 \left(\frac{d\sigma}{d\Omega} \right)^{\text{HOES}}, \quad (1)$$

where KF is a kinematical factor, depending on the masses and energies of the detected particles. The experimental spectator momentum distribution $|\Phi(\mathbf{p}_s)|^2$ is linked to the p - n relative motion inside deuteron (Lamia et al. 2012a), where $(d\sigma/d\Omega)^{\text{HOES}}$ is the half-off-energy-shell (HOES) cross-section of the reaction of astrophysical interest (Mukhamedzhanov 2011).

According to the THM premises, the Coulomb barrier is overcome in the entrance channel; thus, the obtained HOES cross-section, $(d\sigma/d\Omega)^{\text{HOES}}$, is essentially the nuclear part of the $^{18}\text{F}(p, \alpha)^{15}\text{O}$ cross-section, without the Coulomb barrier suppression and electron screening enhancement. However, the HOES cross-section is obtained with an arbitrary normalization to be matched to the directly measured cross-sections, so that direct data have to be present at energies appropriate for the normalization procedure. The agreement between the THM and the direct cross-sections at high energies and the subsequent scaling represents a necessary validation of the THM, in view of its application to measurements of reactions of astrophysical interest and constitutes a necessary step also for reactions induced by radioactive ion beams, such as the $^{18}\text{F}(p, \alpha)^{15}\text{O}$.

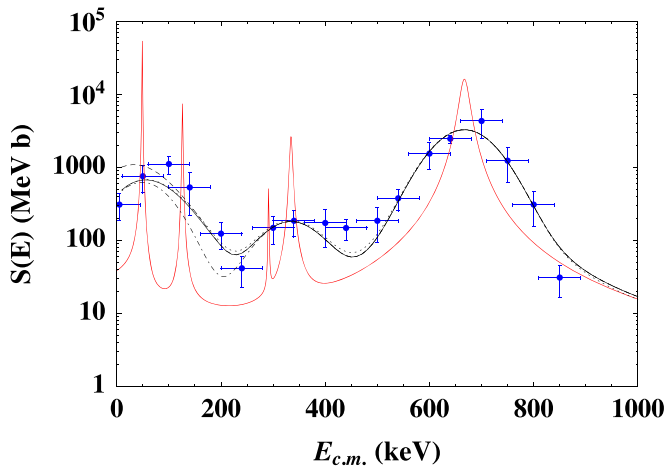


Figure 1. R-matrix analysis of the THM astrophysical factor (blue points), under the assumption of $J^\pi = 3/2^+$ for the 6460 keV ^{19}Ne state as discussed in Cherubini et al. (2015) and Pizzone et al. (2016). The solid black line is the smoothed R-matrix calculation, accounting for a 53 keV energy spread (standard deviation), with parameters given in Table 1. The red line is the corresponding deconvoluted astrophysical factor. The dashed black line is the smoothed R-matrix calculation including the 6417 keV level, while the dotted-dashed line is the smoothed R-matrix calculation, where the 6537 keV is excluded. Finally, the dotted line marks the smoothed R-matrix calculation where the interference signs were changed to $(++)(-+)$.

In recent years, an intensive experimental and theoretical activity has been carried out to upgrade the THM approach, with the aim of making normalization to direct data unnecessary (La Cognata et al. 2009, 2010, 2013; Mukhamedzhanov 2011; Trippella & La Cognata 2017). This is an important step in the application of the THM to reactions involving unstable nuclei, since in many cases no direct data exist for normalization, chiefly in the case of reactions induced by neutrons on unstable nuclei. This novel perspective also has the advantage of fully accounting for HOES effects and of allowing us to extend the THM reach by using more advanced nuclear reaction models, such as the Distorted Wave Born Approximation and the Continuum-Discretised Coupled Channel approaches (La Cognata et al. 2009; Mukhamedzhanov 2011).

Two experimental runs were performed by applying the THM to the $^2\text{H}(^{18}\text{F}, \alpha)^{15}\text{O}n$ reaction and we refer for further details on the experiments and data analysis to Cherubini et al. (2015) for the first run (performed at CNS-RIKEN, hereby RIKEN run) and to Pizzone et al. (2016) for the second run (performed at Texas A&M University, hereby TAMU run). Both data sets are in agreement with each other within the experimental errors and can offer complementary information with respect to the direct measurements. In Figure 1, the average of the two data sets, weighted over the respective experimental errors, is reported as blue symbols, together with the statistical as well as the normalization errors. The horizontal error bar marks instead the energy uncertainty, essentially linked to the binning chosen in the data reduction (see Cherubini et al. 2015; Pizzone et al. 2016 for more details).

3. R-matrix Analysis of the $^{18}\text{F}(p, \alpha)^{15}\text{O}$ THM S-factor

Guided by the recent work by Bardayan et al. (2015), we have performed an R-matrix analysis of the THM data (Cherubini et al. 2015; Pizzone et al. 2016), with the aim to check the compatibility of the THM S-factor with this recent R-matrix calculation, discussing, updating, combining, and

Table 1
Parameters of the R-matrix Calculation (Red Line) in Figure 1

E_{res} (keV)	E_x (keV)	J^π	Γ_p (keV)	Γ_α (keV)
-124	6286	$1/2^+$	83.5^a	11.6
7	6417	$3/2^-$	$1.6 \cdot 10^{-41}$	0.5
29	6440	$1/2^-$	$3.8 \cdot 10^{-19}$	220
49	6460	$3/2^+$	$2.3 \cdot 10^{-13}$	0.9
126	6537	$7/2^+$	$7.1 \cdot 10^{-8}$	1.5
291	6702	$5/2^+$	$2.4 \cdot 10^{-5}$	1.2
334	6745	$3/2^-$	$2.2 \cdot 10^{-3}$	5.2
665	7075	$3/2^+$	15.2	23.8
1461	7872	$1/2^+$	55	347

Note. Resonance energies, corresponding levels in ^{19}Ne , spin-parities, Γ_p and Γ_α are reported, respectively. The 7 keV state is also shown, even though it is not needed to reproduce the THM data.

^a Since this is a sub-threshold resonance, the ANC in $\text{fm}^{1/2}$ is cited.

Table 2
Reaction Rate as a Function of the Temperature

T_9	R_{ij} ($\text{cm}^3 \text{mol}^{-1} \text{s}^{-1}$)
0.007	2.49673×10^{-28}
0.008	1.47096×10^{-26}
0.009	4.68148×10^{-25}
0.01	9.39356×10^{-24}
0.015	1.15888×10^{-18}
0.02	5.63177×10^{-15}
0.03	3.6577×10^{-11}
0.05	3.57743×10^{-8}
0.1	0.000260867
0.15	0.0187306
0.2	0.168753
0.25	1.03239
0.3	5.96964
0.35	26.049
0.4	87.1969
0.45	249.303
0.5	654.916
0.6	3668.36
0.7	14842.5
0.8	44314.9
0.9	104398
1	206150

analyzing the most recent direct and indirect results on the $^{18}\text{F}(p, \alpha)^{15}\text{O}$ reaction, excluding the THM data. The THM $S(E)$ factor is shown as blue symbols in Figure 1, and is taken from Pizzone et al. (2016) (the average of the RIKEN and TAMU run data).

The resonance parameters used in the R-matrix analysis are given in Table 1. The same states as in Bardayan et al. (2015) were considered, with the corresponding parameters being taken from Table 2. However, to reproduce THM data, some changes have been proven necessary, following the discussion in Cherubini et al. (2015) and Pizzone et al. (2016). In detail, the best-fit curve (shown as a solid black line in Figure 1) is achieved by assuming the $(++)((++))$ interference pattern, according to the notation in Figure 3 of Bardayan et al. (2015), excluding the 7 keV resonance, attributable to the occurrence of a $3/2^-$ state of ^{19}Ne at 6417 keV energy, and introducing a $7/2^+$ state of ^{19}Ne at 6537 keV, as remarked in Cherubini et al. (2015) and Pizzone et al. (2016). The $(++)((++))$ notation is

used to point out that the relative interference signs between the -124 and 1461 keV resonances is $(++)$ (first pair) and the ones of the 47 and 665 keV resonances is $(++)$ as well (second pair). The corresponding astrophysical factor, given by the red line in Figure 1, has been smeared to account for the experimental energy resolution, which has been evaluated in Cherubini et al. (2015) and equals 53 keV (standard deviation), leading to the solid black line. For 18 degrees of freedom, a reduced $\chi^2 = 1.5$ is obtained in this case.

Alternative solutions were checked, to see if they cannot be excluded based on THM data. First, we have performed the same calculation including the 6417 keV state. After smoothing, the dashed black line in Figure 1 is obtained, resulting in a reduced $\chi^2 = 3.1$ for 18 degrees of freedom. The incompatibility of the THM experimental S-factor with the calculation including the 7 keV resonance can be quantitatively estimated if the deviation, with respect to the assessed uncertainty, is calculated at 5 keV, the experimental point closer to the resonance centroid. Simple algebra leads to a disagreement at the 5.5σ level, making us confident that, in this case, the adjustment of the parameters in Bardayan et al. (2015) is reasonable. However, since our result is based on a single experimental point, more work is mandatory to rule out a contribution from this level. This resonance causes an increase of the smoothed astrophysical factor below 100 keV (see Figure 1), which is incompatible with THM results, the reduced χ^2 being a factor of two larger in this last case. Such a result is consistent with the absence of observation of the mirror state in the reanalysis of the $^{15}\text{N}(\alpha, \alpha)^{15}\text{N}$ cross-section (Bardayan et al. 2005).

Focusing on the 126 keV resonance, which is mentioned by Cherubini et al. (2015) and Pizzone et al. (2016) but not included in the R-matrix calculation by Bardayan et al. (2015), the corresponding smeared S-factor is shown as a dotted-dashed black line in Figure 1. In this case, a reduced $\chi^2 = 1.8$ is deduced, larger than the best-fit case (namely, 1.5) but probably not different enough to definitely claim its occurrence. Finally, the sensitivity of the THM S-factor on the interference pattern has been tested, by switching from the $(++)$ $(++)$ relative signs to the $(++)$ $(-+)$ combination, that is, assuming constructive interference between the $3/2^+$ states. We focus on these patterns because they involve states observed in the THM measurements (Cherubini et al. 2015; Pizzone et al. 2016). After including energy resolution effects, the dotted curve in Figure 1 is retrieved, almost indistinguishable from the best-fit curve (solid black line). Therefore, the energy resolution affecting the present THM S-factor is not enough to pick the most likely interference pattern, energy resolution washing out eventual differences. Similar results are obtained if the $(-+)$ $(++)$ and $(-+)$ $(-+)$ combinations are used, because of the poor energy resolution affecting the THM experimental points. Other interference schemes were not taken into account since they are presently excluded (see the discussion in Bardayan et al. 2015). This result supports further THM measurements of the $^{18}\text{F}(p, \alpha)^{15}\text{O}$ THM S-factor, which might prove very useful to single out the most likely interference pattern since it makes it possible to reach the energies of astrophysical interest, at odds with present-day direct measurements. It is also worth noting that, because of the energy resolution, the weak 6440 and 6702 keV states were not reported in Cherubini et al. (2015) and Pizzone et al. (2016). Energy smearing, in fact, almost completely suppresses their contribution in comparison

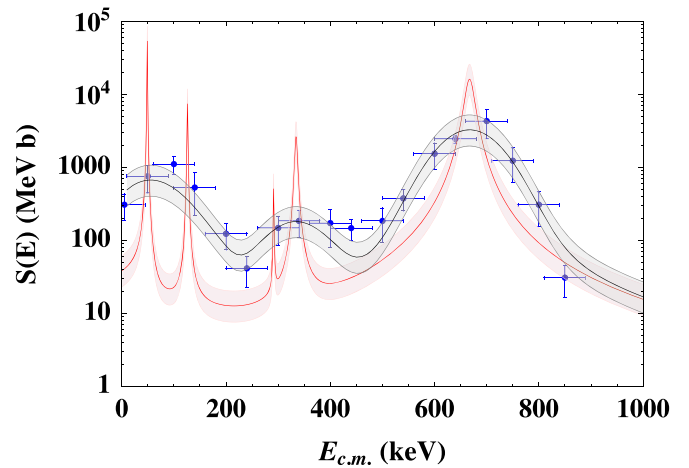


Figure 2. R-matrix analysis of the THM astrophysical factor (blue points) as in Figure 1. The evaluated uncertainty in the R-matrix fit is reported as a shadowed gray area and as a red band for the corresponding deconvoluted S(E)-factor.

to that of the neighboring more intense resonances. Therefore, future THM measurements need to aim at improved energy resolution, even if the quality of radioactive ion beams available today set a limit at the resolution that can be achieved.

For the best-fit curve, we have performed an error estimate by fitting the upper and lower limits set by the uncertainties affecting the experimental data. The resulting error bands affecting the R-matrix calculations are reported in Figure 2 as a shadowed gray band and as a red band for the smoothed and the deconvoluted S(E)-factor, respectively.

4. Calculation of the Reaction Rate

The reaction rate of the THM deconvoluted astrophysical factor, given by the red line of Figure 1, has been calculated using standard equations (Iliadis 2007). The resulting reaction rate is shown in the upper panel of Figure 3 as a function of the temperature, expressed in units of 10^9 K ($T_9 = T/10^9$ K), and listed in Table 2. For comparison, in the lower panel of the same figure, the ratio of the THM reaction rate to the one reported in the JINA REACLIB database (Cyburt et al. 2010) is also displayed. The latter is the interpolation of the Iliadis et al. (2010) reaction rate using a standard formula (Cyburt et al. 2010), differing at most by 10% from the original calculation. We are juxtaposing the THM rate with the Cyburt et al. (2010) one since the latter is commonly used in novae modeling. In the temperature region of interest for astrophysics, $0.1 \lesssim T_9 \lesssim 0.5$, an increase in the reaction rate ratio is observed, compatible with the results by Bardayan et al. (2015). The absence of the 7 keV resonance, whose occurrence is not supported by THM data, determines a decrease of the reaction rate ratio below such a temperature, even if the astrophysical consequences of this modification are likely to be negligible. The uncertainties arising from the present measurement are fully accounted for and reported in Figure 3 as a shadowed band.

The extracted reaction rate has significant astrophysical implications, especially in the novae temperature range, where a larger rate with respect to Cyburt et al. (2010) and Bardayan et al. (2002) is calculated.

Table 3
Mass-averaged Composition in the Nova Ejecta (CNOF-group Elements)

	Model A	Model B	Model C	Model D	Model D'	Model E
WD	CO	CO	ONe	ONe	ONe	ONe
$M_{\text{wd}} (M_{\odot})$	1	1.15	1.15	1.25	1.25	1.35
Reference	This Work	This Work	This Work	This Work	Iliadis et al. (2010)	This Work
^{12}C	4.52E-2	4.76E-2	2.28E-2	2.61E-2	2.61E-2	2.21E-2
^{13}C	1.10E-1	7.87E-2	2.15E-2	2.54E-2	2.55E-2	1.56E-2
^{14}N	1.18E-1	1.33E-1	3.36E-2	4.15E-2	4.15E-2	5.47E-2
^{15}N	9.63E-3	3.66E-2	3.57E-2	5.66E-2	5.66E-2	1.07E-1
^{16}O	2.40E-1	2.23E-1	1.09E-1	6.12E-2	6.11E-2	5.97E-3
^{17}O	4.74E-3	1.15E-2	2.90E-2	3.67E-2	3.68E-2	4.05E-2
$^{18}\text{O}^{\text{a}}$	3.09E-7	5.67E-7	1.49E-6	2.09E-6	4.59E-6	8.81E-6
$^{18}\text{F}^{\text{a}}$	7.14E-7	1.29E-6	3.48E-6	4.82E-6	1.03E-5	1.98E-5
^{19}F	2.03E-8	1.86E-8	3.62E-8	1.19E-7	1.40E-7	1.42E-6

Note.

^a Values correspond to 1 hr after peak temperature was achieved in the envelope.

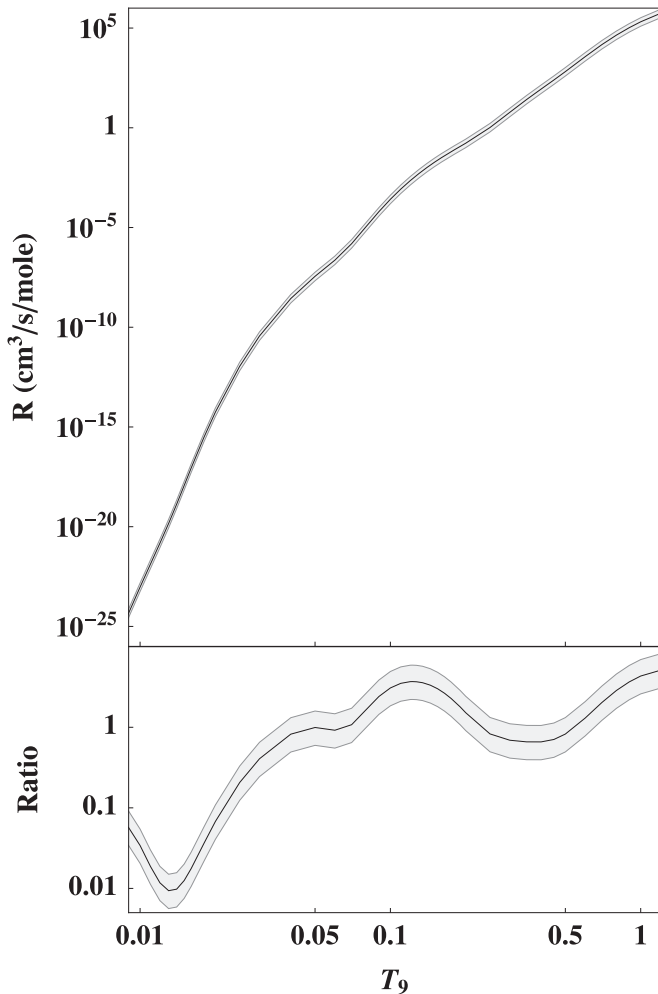


Figure 3. Upper panel: $^{18}\text{F}(p, \alpha)^{15}\text{O}$ reaction rate calculated using the deconvoluted THM S-factor (red line of Figure 1). Lower panel: ratio of the THM reaction rate to the one reported in the JINA REACLIB database (Cyburt et al. 2010). In both plots, the uncertainties of the reaction rate are represented as a shadowed band.

5. Astrophysical Implications

To examine the impact of the new determination of the $^{18}\text{F}(p, \alpha)^{15}\text{O}$ rate on nova nucleosynthesis, a series of one-dimensional, hydrodynamic simulations have been performed

with the SHIVA code (José & Hernanz 1998; José 2016). Two models of $1.25 M_{\odot}$ oxygen–neon white dwarfs, accreting H-rich material from the stellar companion at a rate of $2 \times 10^{-10} M_{\odot} \text{ yr}^{-1}$, have been computed with identical input physics except for the prescription adopted for the $^{18}\text{F}(p, \alpha)^{15}\text{O}$ rate (Models D and D'). While no change on the dynamical properties of the explosion is found (e.g., peak temperature attained, amount of mass ejected), Table 3 reveals important differences in the chemical composition of the ejected matter, with a net reduction in the mean ^{18}F content by a factor of $^{18}\text{F}_{\text{D}'} / ^{18}\text{F}_{\text{D}} \sim 2.1$, which reduces previous estimates of the detectability distance of the 511 keV annihilation line by γ -ray satellites by a factor $\sim \sqrt{2}$. Note, as well, that larger amounts of ^{18}O and a net reduction of ^{19}F by a $\sim 20\%$ are also found when the new $^{18}\text{F}(p, \alpha)^{15}\text{O}$ rate, rather than the prescription reported in Iliadis et al. (2010), is used.

Four additional models (Models A, B, C, and E), covering a wide range of masses for the accreting white dwarf (i.e., two carbon–oxygen white dwarfs of $1 M_{\odot}$ and $1.15 M_{\odot}$, and two oxygen–neon white dwarfs of $1.15 M_{\odot}$, and $1.35 M_{\odot}$), have also been computed. Results are summarized as well in Table 3. All of these models result in a net reduction of the final ^{18}F content when compared with models computed with the Iliadis et al. (2010) rate.

6. Concluding Remarks

In this work, we have assessed the impact of the recent indirect measurement of the $^{18}\text{F}(p, \alpha)^{15}\text{O}$ cross-section by means of the THM (Cherubini et al. 2015; Pizzone et al. 2016) on the synthesis of carbon, nitrogen, oxygen, and fluorine isotopes in novae, as well as the changes of the dynamics of the explosion. This has been achieved by inserting the calculated reaction rate into the SHIVA code (José & Hernanz 1998; José 2016) and comparing the output with the results obtained by considering the $^{18}\text{F}(p, \alpha)^{15}\text{O}$ reaction rate of Iliadis et al. (2010).

To calculate the reaction rate, the THM data in Cherubini et al. (2015) and Pizzone et al. (2016) could not be used as they are because of the energy resolution affecting the indirect astrophysical factor. Therefore, based on the recent work of Bardayan et al. (2015), we have performed an R-matrix analysis of the THM S(E) to deduce the infinite resolution astrophysical factor. In this way, we have been able to supply


a reaction rate devoid of experimental effects, which can be juxtaposed to other results in the literature, consistently propagating the uncertainties on energy and on $S(E)$. From this analysis, it turns out that THM data tend to disfavor the contribution of the 6417 keV state of ^{19}Ne , while supporting the occurrence of the 126 keV resonance in the $^{18}\text{F}(p, \alpha)^{15}\text{O}$ astrophysical factor.

As a consequence of the THM $S(E)$, the reaction rate shows an increase right at novae temperatures (peak values of $T_9 \sim 0.1\text{--}0.5$). While the explosion dynamics is not affected, the chemical composition of the ejected material shows significant differences when the THM reaction rate is used. In particular, the ^{18}F content in the nova ejecta reported in this work demonstrates a factor of about 2 decrease, reducing the detectability distance by a factor of about 1.4.

Software: SHIVA (José & Hernanz 1998; José 2016).

ORCID iDs

M. La Cognata  <https://orcid.org/0000-0002-1819-4814>

J. José  <https://orcid.org/0000-0002-9937-2685>

M. Hernanz  <https://orcid.org/0000-0002-8651-7910>

References

- Bardayan, D. W., Batchelder, J. C., Blackmon, J. C., et al. 2002, *PhRvL*, **89**, 262501
- Bardayan, D. W., Chipps, K. A., Ahn, S., et al. 2015, *PhLB*, **751**, 311
- Bardayan, D. W., Kozub, R. L., & Smith, M. S. 2005, *PhRvC*, **71**, 018801
- Beer, C. E., Laird, A. M., Murphy, A., St. J., et al. 2011, *PhRvC*, **83**, 042801
- Cherubini, S., Gulino, M., Spitaleri, C., et al. 2015, *PhRvC*, **92**, 015805
- Clayton, D. D. 1981, *ApJL*, **244**, L97
- Clayton, D. D., & Hoyle, F. 1974, *ApJL*, **187**, L101
- Coc, A., Hernanz, M., José, J., & Thibaud, J. P. 2000, *A&A*, **357**, 561
- Cyburt, R. H., Amthor, A. M., Ferguson, R., et al. 2010, *ApJS*, **189**, 240
- De Sereville, N., Angulo, C., A. Coc, A., et al. 2009, *PhRvC*, **79**, 015801
- Diehl, R. 2010, AIP Conf. Proc. 1269, The 10th International Symposium on Origin of Matter and Evolution of Galaxies: OMEG-2010, ed. I. Tanihara et al. (Melville, NY: AIP), 144
- Gómez-Gomar, J., Hernanz, M., José, J., & Isern, J. 1998, *MNRAS*, **296**, 913
- Gulino, M., Spitaleri, C., Tang, X., et al. 2013, *PhRvC*, **87**, 12801
- Harris, M. J., Naya, J. E., Teegarden, B. J., et al. 1999, *ApJ*, **522**, 424
- Hernanz, M. 2008, in *Classical Novae*, ed. M. F. Bode & A. Evans (2nd ed.; Cambridge: Univ. Press), 252
- Hernanz, M. 2014, in *ASP Conf. Ser. 490, Stella Novae: Past and Future Decades*, ed. P. A. Woudt & V. A. R. M. Ribeiro (San Francisco, CA: ASP), 319
- Hernanz, M., & José, J. 2004, in 5th INTEGRAL Workshop “the INTEGRAL Universe” (ESA SP-552), ed. V. Schönfelder, G. Lichti, & C. Winkler (Noordwijk: ESA), 95
- Hernanz, M., José, J., Coc, A., et al. 1999, *ApJL*, **526**, L97
- Hernanz, M., Smith, D. M., Fishman, J., et al. 2000, in AIP Conf. Proc. 510, The Fifth Compton Symposium, ed. M. McConnell & J. M. Ryan (Melville, NY: AIP), 82
- Iliadis, C. 2007, *Nuclear Physics of Stars* (New York: Wiley)
- Iliadis, C., Longland, R., Champagne, A. E., et al. 2010, *NuPhA*, **841**, 31
- José, J. 2016, *Stellar Explosions: Hydrodynamics and Nucleosynthesis* (Boca Raton, FL, London: CRC/Taylor and Francis)
- José, J., & Hernanz, M. 1998, *ApJ*, **494**, 680
- José, J., & Hernanz, M. 2007, *JPhG*, **34**, R431
- José, J., & Shore, S. N. 2008, in *Classical Novae*, ed. M. F. Bode & A. Evans (2nd ed.; Cambridge: Univ. Press), 121
- La Cognata, M., Goldberg, V., Mukhamezhanov, A. M., et al. 2009, *PhRvC*, **80**, 012801
- La Cognata, M., Palmerini, S., Spitaleri, C., et al. 2015, *ApJ*, **805**, 128
- La Cognata, M., Spitaleri, C., Mukhamezhanov, A., et al. 2010, *ApJ*, **723**, 1512
- La Cognata, M., Spitaleri, C., Trippella, O., et al. 2013, *ApJ*, **777**, 143
- Laird, A., Parikh, A., Murphy, A., St. J., et al. 2013, *PhRvL*, **110**, 032502
- Lamia, L., La Cognata, M., Spitaleri, C., et al. 2012a, *PhRvC*, **85**, 025805
- Lamia, L., Spitaleri, C., La Cognata, M., et al. 2012b, *A&A*, **541**, 158
- Lamia, L., Spitaleri, C., Pizzone, R. G., et al. 2013, *ApJ*, **768**, 65
- Lamia, L., Spitaleri, C., Tognelli, E., et al. 2015, *ApJ*, **811**, 99
- Leising, M. D., & Clayton, D. D. 1987, *ApJ*, **323**, 159
- Livio, M., Mastichiadis, A., Oegelman, H., et al. 1992, *ApJ*, **394**, 217
- Mathews, T. G., Smith, D. M., & Hernanz, M. 2006, *BAAS*, **38**, 344
- Mukhamedzhanov, A. 2011, *PhRvC*, **84**, 044616
- Palmerini, S., Sergi, S., La Cognata, M., et al. 2013, *ApJ*, **764**, 128
- Pizzone, R. G., Roeder, B., McCleskey, M., et al. 2016, *EPJA*, **52**, 24
- Pizzone, R. G., Spartá, R., Bertulani, C., et al. 2014, *ApJ*, **786**, 112
- Pizzone, R. G., Tumino, A., Degl’Innocenti, S., et al. 2005, *A&A*, **438**, 779
- Spitaleri, C. 1991, in *Problems of Fundamental Modern Physics II*, ed. R. Cherubini, P. Dalpiaz, & B. Minetti (Singapore: World Scientific), 21
- Spitaleri, C., La Cognata, M., Lamia, L., et al. 2016, *EPJA*, **52**, 77
- Spitaleri, C., Lamia, L., Puglia, S. M. R., et al. 2014, *PhRvC*, **90**, 035801
- Starrfield, S., Iliadis, C., & Hix, W. R. 2008, in *Classical Novae*, ed. M. F. Bode & A. Evans (2nd ed.; Cambridge: Univ. Press), 77
- Starrfield, S., Iliadis, C., & Hix, W. R. 2016, *PASP*, **128**, 051001
- Suzuki, A., & Shigeeyama, T. 2010, *ApJL*, **723**, L84
- Tribble, R. E., Bertulani, C., La Cognata, M., et al. 2014, *RPPH*, **77**, 106901
- Trippella, O., & La Cognata, M. 2017, *ApJ*, **837**, 41
- Tumino, A., Spartá, R., Spitaleri, C., et al. 2014, *ApJ*, **785**, 96